Available online at www.sciencedirect.com
SCIENCE DIRECT®
Pergamon
Acta Materialia 51 (2003) 887–898
Acta MATERIALIA
www.actamat-journals.com

Transformations of grain boundary dislocation pile-ups in nano- and polycrystalline materials

A.A. Fedorov, M.Yu. Gutkin *, I.A. Ovid'ko

Institute of Problems of Mechanical Engineering, Russian Academy of Sciences Bolshoj 61, Vas. Ostrov, St. Petersburg 199178, Russia

Received 20 March 2002; received in revised form 16 September 2002; accepted 16 September 2002

Abstract

A theoretical model is suggested which describes several types of transformations of grain boundary dislocation pile-ups at triple junctions of grain boundaries in (super) plastically deformed nanocrystalline and polycrystalline materials. Ranges of parameters of defect configurations are revealed at which the transformations considered are energetically favourable. The role of transformations of grain boundary dislocation pile-ups at triple junctions of grain boundaries in plastic deformation processes in nanocrystalline and polycrystalline materials is discussed with special attention being paid to the influence of such transformations on competition between different deformation mechanisms in nanocrystalline materials.

Keywords: Deformation; Grain boundaries; Dislocations; Nanostructures

1. Introduction

Transformations of grain boundary defects strongly influence both the structure and the properties of solids; see, e.g., [1–18]. In particular, the grain boundary sliding which occurs via motion of grain boundary dislocations (GBDs) crucially affects the deformation behavior of polycrystalline and nanocrystalline materials [1–12]. Thus, it has been well established that grain boundary sliding is mainly responsible for superplasticity which is quite common for fine-grained metals, intermetallics and ceramics at specific temperature and strain rate conditions; see, e. g., [1,2]. The features of grain boundary sliding strongly depend on triple junctions of grain boundaries [19–24]. In particular, the effects of triple junctions on the deformation behavior are of utmost importance in nanocrystalline materials where the volume fraction of triple junctions is extremely high. At present, the role of triple junctions in plastic deformation in polycrystalline and nanocrystalline materials is not understood in detail due to difficulties in experimental identification of the effects of triple junctions that often exhibit themselves in combination with those of "conventional" grain boundaries [19]. In these circumstances, theoretical modelling of transformations of GBDs, that occur at triple junc-

* Corresponding author. Fax: +7-812-321-4771.
E-mail address: gutkin@def.ipme.ru (M.Yu. Gutkin).

1359-6454/03/$30.00
doi:10.1016/S1359-6454(02)00433-0

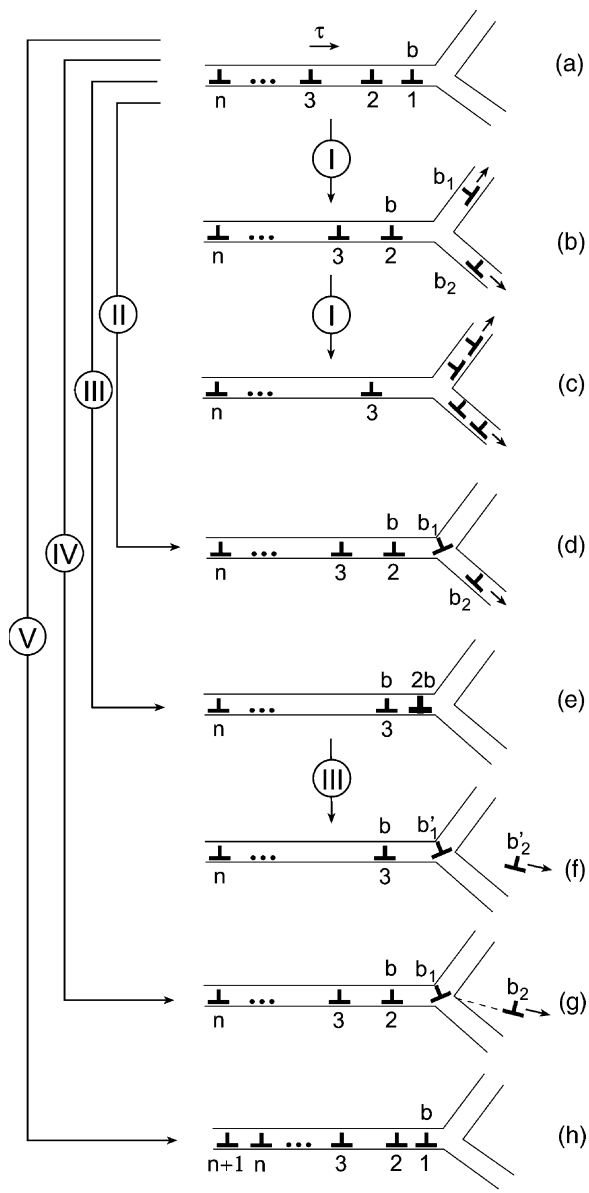

Fig. 1. Transformations of grain boundary dislocation pile-ups at triple junction of grain boundaries. (a) Dislocation pile-up stops at triple junction. (b) Head dislocation of pile-up splits into two mobile dislocations that move along adjacent grain boundaries. (c) Second head dislocation of pile-up splits into two mobile dislocations that move along adjacent grain boundaries. (d) Head dislocation of pile-up splits into immobile grain boundary dislocation that stays at triple junction and mobile grain boundary dislocation moving along an adjacent boundary. (e) Two dislocations converge into a dislocation with Burgers vector 2***b***. (f) Dislocation with Burgers vector 2***b*** splits into immobile grain boundary dislocation that stays at triple junction and mobile lattice dislocation that moves in grain interior. (g) Head dislocation of pile-up splits into immobile grain boundary dislocation that stays at triple junction and mobile partial dislocation which moves in grain interior, with stacking fault (dashed line) formed behind it. (h) New dislocation joins to the stopped dislocation pile-up.

tions is of high interest for understanding the relationships between the microstructure and the mechanical properties of materials. The main aim of this paper is to suggest a theoretical model which describes transformations of GBD pile-ups at triple junctions of grain boundaries and their influence on grain boundary sliding in (super) plastically deformed polycrystalline and nanocrystalline materials. The results of the model are used here for a discussion of the non-conventional Hall-Petch relationship as well as homogeneous and inhomogeneous regimes of plastic flow in nanocrystalline materials.

2. Transformations of grain boundary dislocation pile-ups at triple junctions. Energetic characteristics

Let us consider a GBD pile-up generated under the action of mechanical load in a grain boundary in a plastically deformed nanocrystalline or polycrystalline sample. Mechanical-load-induced motion of the GBD pile-up is stopped by a triple junction of grain boundaries (Fig. 1a). In these circumstances, there are five basic ways of evolution of the GBD pile-up:

I The head dislocation (with Burgers vector ***b***) of the pile-up splits into the two dislocations (with Burgers vectors $\boldsymbol{b}_1$ and $\boldsymbol{b}_2$, respectively) that move along the adjacent grain boundaries (Fig. 1b). This process may repeatedly occur resulting in the consequent splitting of even all the dislocations that compose the pile-up (Fig. 1c).

II The head dislocation of the pile-up splits into an immobile GBD with Burgers vector $\boldsymbol{b}_1$, which stays at the triple junction, and a mobile

GBD with Burgers vector $\boldsymbol{b}_2$, which moves along one of adjacent grain boundaries (Fig. 1d).

III Two (or more) GBDs each is characterized by Burgers vector $\boldsymbol{b}$ converge into a dislocation with Burgers vector $\boldsymbol{B} = 2\boldsymbol{b}$ having magnitude close to the crystal lattice parameter (Fig. 1e). Then the resultant dislocation splits into a mobile lattice dislocation with Burgers vector $\boldsymbol{b}'_2$, which moves to the adjacent grain interior, and an immobile GBD with Burgers vector $\boldsymbol{b}'_1$, which stays at the triple junction (Fig. 1f).

IV The head dislocation of the pile-up splits into an immobile GBD (with Burgers vector $\boldsymbol{b}_1$) that stays at the triple junction and a mobile partial dislocation (with Burgers vector $\boldsymbol{b}_2$) that moves in grain interior, in which case a stacking fault is formed behind the moving patial dislocation (Fig. 1g).

V The pile-up is immobile. It accumulates new GBDs generated under the action of mechanical load (Fig. 1h). This process precedes one of the processes (I)–(IV).

It is worth noting that the suggested model (Fig. 1) refers to a rather specialized picture. For example, consideration of accommodating diffusion processes and grain boundary migration is omitted here, because of mathematical complications associated with analysis of the combined effects of grain boundary sliding, migration and diffusion. However, results of the model are supposed to clarify the key tendencies related to the role of triple junctions in grain boundary sliding processes and can serve as a basis for further theoretical and experimental investigations of grain boundary sliding and its contribution to plastic deformation in nano- and polycrystalline materials.

Now let us compare energetic characteristics of the processes (I)–(IV), using the model suggested (Fig. 1). This will allow us to select the most effective, energetically favourable process(es) occurring at triple junctions of grain boundaries in plastically deformed nanocrystalline and polycrystalline materials. For these purposes, let us model a GBD pile-up at a triple junction of grain boundaries as follows. The pile-up consists of n ($n > 1$) GBDs each characterized by the Burgers vector $\boldsymbol{b}$ (Fig. 1a). The pile-up is under the action of the shear stress τ. The processes (I)–(IV) result, in particular, in the splitting of the head dislocation of the pile-up into the two dislocations. The geometry of the splitting is characterized by α_1 and α_2 being the angles between the Burgers vector $\boldsymbol{b}$ of the pre-existent head dislocation and the Burgers vectors of, respectively, the first and second resultant dislocations.

For definiteness, we will start our analysis with consideration of the process (I). In this process, the head dislocation of the pile-up (Fig. 1a) splits into the two dislocations which move along the adjacent grain boundaries, namely the first and second resultant dislocations with Burgers vectors $\boldsymbol{b}_1$ and $\boldsymbol{b}_2$, respectively (Fig. 1b). The angles α_1 and α_2 in the situation discussed also play the role of the angles between grain boundary planes.

The splitting of the head dislocation is energetically favourable, if the energy (per unit of the dislocation length) E_2 of the defect configuration resulted from the splitting (Fig. 1b) is lower than the energy E_1 of the pre-existent defect configuration (Fig. 1a). That is, the splitting occurs as an energetically favourable process, provided

$$\Delta E = E_2 - E_1 < 0. \tag{1}$$

The energy of the pre-existent defect configuration (Fig. 1a) can be written as follows:

$$E_1 = E'_{n-1} + E^s + E^{\text{int}}, \tag{2}$$

Here E'_{n-1} denotes the total energy of $(n-1)$ GBDs that belong to the pile-up and remain unchanged during the transformation in question (here and in the following we shall denote such GBDs as "unchanged GBDs", for ease of reference), E^s the self energy of the head GBD, E^{int} the energy that characterizes the elastic interaction of the head dislocation and the unchanged GBDs. The assumption that the positions of the $(n-1)$ GBDs in the pile-up remain unchanged may look too strong. However, during the process of the transformations of the head GBD, when the "new" dislocations move within a very small region (say, some b) near the triple junction, this assumption seems to be reasonable.

The energy of the defect configuration resulted from the splitting (Fig. 1b) is given by:

$$E_2 = E'_{n-1} + E_1^s + E_2^s + E_1^{\text{int}} + E_2^{\text{int}} + E_{1-2}^{\text{int}} - A_1 - A_2. \quad (3)$$

Here E_1^s (E_2^s) denotes the self energy of the first (second) resultant dislocation, E_1^{int} (E_2^{int}) the energy that characterizes the elastic interaction between the unchanged GBDs and the first (second) resultant dislocation, E_{1-2}^{int} the energy that characterizes the elastic interaction between the first and second resultant dislocations, A_1 (A_2) the mechanical work carried out by the stress τ to transfer the first (second) resultant dislocation to its final position shown in Fig. 1b. The energy difference ΔE then reads:

$$\Delta E = E_1^s + E_2^s - E^s + E_1^{\text{int}} + E_2^{\text{int}} + E_{1-2}^{\text{int}} - E^{\text{int}} - A_1 - A_2. \quad (4)$$

The self energies, E^s, E_1^s and E_2^s, figuring in eq. (4) can be written in the standard way [25] as follows:

$$\frac{E^s}{b^2} = \frac{E_1^s}{b_1^2} = \frac{E_2^s}{b_2^2} = \frac{G}{4\pi(1-\nu)}\left(\ln\frac{R}{r_c} + Z\right), \quad (5)$$

where G denotes the shear modulus, ν the Poisson ratio, R the screening length of dislocation stress fields, r_c the dislocation core radius, and Z the factor taking into account the contribution of dislocation core to the self energy.

Formulae for A_1 and A_2 are given in the standard way [25] by:

$$\frac{A_1}{b_1\cos 2\alpha_1} = \frac{A_2}{b_2\cos 2\alpha_2} = \tau w, \quad (6)$$

where w is the distance moved by each of the resultant dislocations along the corresponding grain boundary (Fig. 1b). For simplicity, we assume w to be the same for both the resultant dislocations.

Let us consider the energy terms E_{1-2}^{int}, E_1^{int} and E_2^{int}. According to our calculations presented in Appendix A, these terms are given by:

$$E_1^{\text{int}} = Dbb_1 \sum_{i=2}^{n} \Psi(\alpha_1, x_{1i}, y_{1i}), \quad (7)$$

$$E_2^{\text{int}} = Dbb_2 \sum_{i=2}^{n} \Psi(\alpha_2, x_{2i}, y_{2i}), \quad (8)$$

$$E_{1-2}^{\text{int}} = Db_1b_2\Psi(\alpha_1 + \alpha_2, x_0, y_0), \quad (9)$$

where

$$\Psi(\alpha,x,y) = \frac{\cos\alpha}{2}\ln\frac{R^2}{x^2+y^2} - \frac{y(x\sin\alpha + y\cos\alpha)}{x^2+y^2} \quad (10)$$

Here the denotations $D = G/[2\pi(1-\nu)]$, $x_0 = w - w\cos(\alpha_1 + \alpha_2)$, $y_0 = -w\sin(\alpha_1 + \alpha_2)$, $x_{1i} = w - x_i\cos\alpha_1$, $y_{1i} = -x_i\sin\alpha_1$, $x_{2i} = w - x_i\cos\alpha_2$, and $y_{2i} = -x_i\sin\alpha_2$ are used, and x_i is the spacing between the ith and "head" dislocations in the pile-up.

The energy E^{int} that characterizes the interaction between the "head" dislocation and the unchanged GBDs may be obtained from eq. (7) in the limiting case $\alpha_1 = 0$, $x_{1i}=x_i$, $y_{1i}=0$, $b_1 = b$, that results in

$$E^{\text{int}} = Db^2 \sum_{i=2}^{n} \ln\frac{R}{x_i}. \quad (11)$$

According to [26], x_i ($i = 2,\ldots,n$) are the roots of the first derivative of the Laguerre polynomial (for details, see Appendix B). From eqs. (2)–(11) we have the following formula for the energy difference ΔE that characterizes the process (I) shown in Fig. 1b:

$$\Delta E_I = \frac{D}{2}(b_1^2 + b_2^2 - b^2)\left(\ln\frac{R}{r_c} + Z\right) - \tau w(b_1\cos 2\alpha_1 + b_2\cos 2\alpha_2) + D\left\{b_1b_2\Psi(\alpha_1 + \alpha_2, x_0, y_0) + b\sum_{i=2}^{n}\left[b_1\Psi(\alpha_1, x_{1i}, y_{1i}) + b_2\Psi(\alpha_2, x_{2i}, y_{2i}) - b\ln\frac{R}{x_i}\right]\right\}. \quad (12)$$

If ΔE_I, given by eq. (12) is lower (larger, respectively) than 0, the process (I) is energetically favourable (unfavourable, respectively).

Now let us turn to a consideration of the energetic characteristics of the processes (II)–(IV) occurring at triple junctions of grain boundaries in

plastically deformed nanocrystalline and polycrystalline materials. By analogy to the scheme considered above for calculating of ΔE_I, we have found the energy differences ΔE_{II}, ΔE_{III} and ΔE_{IV}, characterizing the processes (II), (III) and (IV), respectively.

Using eq. (12) for ΔE_I, it is possible to simplify a formula for ΔE_{II} as follows:

$$\Delta E_{II} = \Delta E_I + Db_1\{b_2[\Psi(\alpha_1 + \alpha_2,x'_0,y'_0) - \Psi(\alpha_1 + \alpha_2,x_0,y_0)] + b\sum_{i=2}^{n}[\Psi(\alpha_1,x'_{1i},y'_{1i}) - \Psi(\alpha_1,x_{1i},y_{1i})]\}, \quad (13)$$

where $x'_0 = w$, $y'_0 = 0$, $x'_{1i} = x_i\cos\alpha_1$, $y'_{1i} = -x_i\sin\alpha_1$, $x'_{2i} = x_i\cos\alpha_2$, and $y'_{2i} = -x_i\sin\alpha_2$.

By analogy, using eq. (13) for ΔE_{II}, it is simple to write a formula for ΔE_{IV} as:

$$\Delta E_{IV} = \Delta E_{II} + \gamma w. \quad (14)$$

The term ΔE_{III} may be obtained as follows. In fact, the process (III) includes two main stages which are (i) the stage of convergence of the first and second dislocations of the initial pile-up which results in a new dislocation with the Burgers vector $2\boldsymbol{b}$, that can be characterized by the energy difference $\Delta E^{(1)}_{III}$, and (ii) the stage of splitting of this new dislocation into two new ones with the Burgers vectors $\boldsymbol{b}'_1$ and $\boldsymbol{b}'_2$, respectively, that can be characterized by the energy difference $\Delta E^{(2)}_{III}$. In doing so, we obtain the term ΔE_{III} as a sum: $\Delta E_{III} = \Delta E^{(1)}_{III} + \Delta E^{(2)}_{III}$. After some algebra, it reads as

$$\Delta E_{III} = \frac{D}{2}(b'^2_1 + b'^2_2 + b^2)\left(\ln\frac{R}{r_c} + Z\right) - \tau w b_2\cos 2\alpha_2 + D\left\{b'_1b'_2\Psi(\alpha_1 + \alpha_2,x'_0,y'_0) + b\sum_{i=3}^{n}\left[b'_1\Psi(\alpha_1,x'_{1i},y'_{1i}) + b'_2\Psi(\alpha_2,x'_{2i},y'_{2i}) - b\ln\frac{R}{x_i}\right]\right\}. \quad (15)$$

It is worth noting that the Burgers vectors $\boldsymbol{b}_1$, $\boldsymbol{b}_2$, $\boldsymbol{b}'_1$ and $\boldsymbol{b}'_2$ of the resultant dislocations figuring in eqs. (12) and (15) and characterizing different dislocation structures (shown in Fig. 1), in general, are different.

3. Results of model

Results of our model considered in previous sections are presented here as numerically calculated dependences of the energy difference ΔE on the parameters, n, α_1, α_2, τ/G, of the defect system which undergoes transformations shown in Fig. 1. These results for the processes (I)–(IV) are as follows.

3.1. Process (I) (see Fig. 1b)

For $n = 5$, and $\tau/G = 0.0002$, 0.002 and 0.01, the dependences $\Delta E_I(w)$ given by eq. (12) are shown in Fig. 2a and b that correspond to $\alpha_1 =$

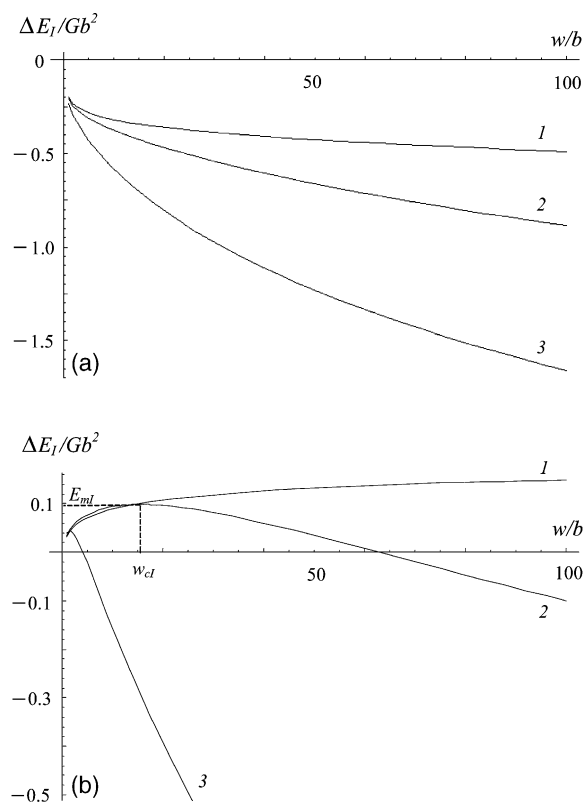

Fig. 2. The energy difference ΔE_I, via the path w of gliding dislocations in the case of $n = 5$ dislocations in the initial pile-up under the external shear stress $\tau/G = 0.0002$, 0.002, and 0.01 (see curves 1, 2, and 3, respectively), for the Burgers vector orientations $\alpha_1 = \alpha_2 = \alpha = 20°$ (a) and 50° (b).

$\alpha_2 = 20°$ and $\alpha_1 = \alpha_2 = 50°$, respectively. As it follows from these dependences, the dislocations behave in rather different manners at small and large values of angles between the adjacent grain boundaries. So, barrierless motion of the resultant dislocations occurs along the grain boundaries at small values of the angles α_1 and α_2. In contrast, for large α_1 and α_2, there is an energy barrier for motion of the resultant dislocations, which is characterized by the barrier height E_{mI} and the critical distance w_{cI} moved by the dislocations (Fig. 2b). Our analysis based on eq. (12) shows that the transition from the barrierless type of the dislocation motion to the barrier one takes place at a critical value of α ($= \alpha_1 = \alpha_2$) $\approx 48°$, which is almost independent on the number n of the grain boundary dislocations composing a pile-up.

Fig. 3 shows variations of dependences $\Delta E_I(w)$ (corresponding to the barrier motion of the resultant dislocations) with n, for $\alpha_1 = \alpha_2 = \alpha = 50°$ and $\tau/G = 0.002$. It is seen from Fig. 3 that both the barrier height E_{mI} and critical distance w_{cI} decrease with rising n.

In Fig. 4, the dependences $E_{mI}(\tau)$ (Fig. 4a) and $w_{cI}(\tau)$ (Fig. 4b) are given for different values of the angles α_1 and α_2. The solid curves correspond here to the condition $\alpha_1 = \alpha_2 = \alpha = (\alpha_1 + \alpha_2)/2$, while the dashed curves correspond to the asymmetric case with $\alpha_1 \neq \alpha_2$. As follows from Fig. 4, the barrier height E_{mI} in the asymmetric case is lower than that in the case with $\alpha_1 = \alpha_2 = \alpha$, while the critical distance w_{cI} is tentatively the same in both the cases. Also, Fig. 4 shows that both E_{mI} and w_{cI} increase with rising the angles α_1 and α_2.

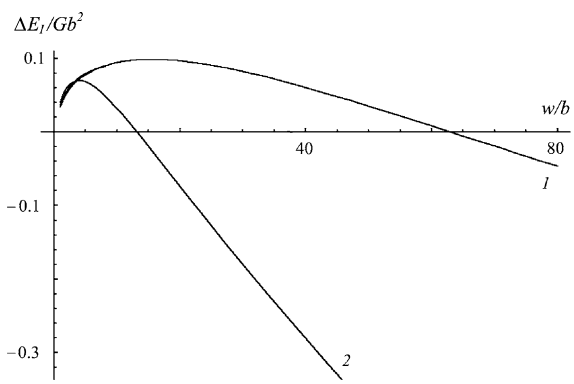

Fig. 3. The energy difference ΔE_I via the path w of gliding dislocations in the case of $n = 5$ (curve 1) and 20 (curve 2) dislocations in the initial pile-up under the external shear stress $\tau/G = 0.002$, for the Burgers vector orientations $\alpha_1 = \alpha_2 = \alpha = 50°$.

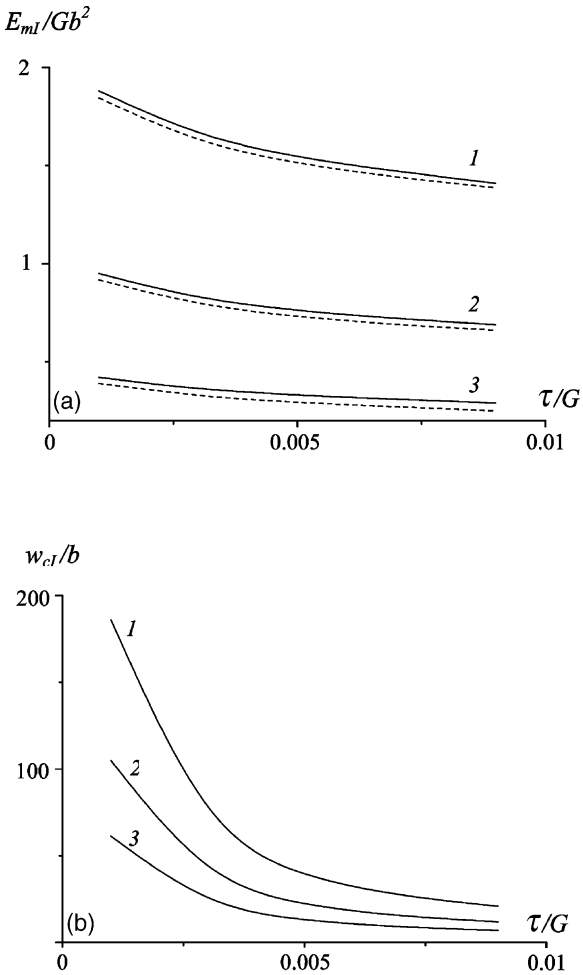

Fig. 4. The energy barrier height E_{mI} (a) and the critical distance w_{cI} (b) via the external shear stress τ for the mean angle $\alpha = (\alpha_1 + \alpha_2)/2 = 65°$ (1), 60° (2), and 55° (3), of the Burgers vector misorientations. The solid lines correspond to the symmetric case with $\alpha_1 = \alpha_2$, while the dashed lines represent the asymmetric case when $\alpha_1 \neq \alpha_2$.

3.2. Process (II) (see Fig. 1d)

For $n = 5$, and $\tau/G = 0.0002$, 0.002 and 0.01, the dependences $\Delta E_{II}(w)$ are presented in Fig. 5a

and b which correspond to $\alpha_1 = \alpha_2 = \alpha = 20°$ and $\alpha_1 = \alpha_2 = \alpha = 50°$, respectively. As with the splitting of the head dislocation into two GBDs moving along adjacent boundaries (the process (I)), the splitting of the pre-existent head dislocation into an immobile GBD and a mobile GBD (Fig. 1d) occurs in the barrierless way at low values of α_1 and α_2, while there is an energetic barrier (characterized by the height E_{mII} and the critical distance w_{cII}) for motion of the resultant lattice dislocation in the case with large values of α_1 and α_2.

Fig. 6 shows variations of the dependences $\Delta E_{II}(w)$ (corresponding to the barrier motion of the lattice dislocation) with the number n of the grain boundary dislocations composing the pile-up, for $\alpha_1 = \alpha_2 = \alpha = 50°$ and $\tau/G = 0.002$. Both the barrier height E_{mII} and critical distance w_{cII} decrease with rising n. Dependences of E_{mII} and

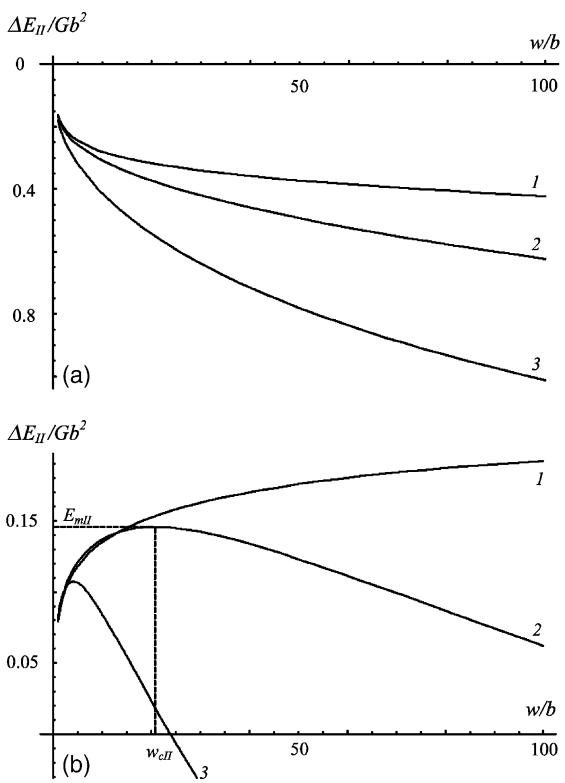

Fig. 5. The energy difference ΔE_{II} via the path w of gliding dislocation in the case of $n = 5$ dislocations in the initial pile-up under the external shear stress $\tau/G = 0.0002$ (1), 0.002 (2), and 0.01 (3), for the Burgers vector orientations $\alpha_1 = \alpha_2 = \alpha = 20°$ (a) and 50° (b).

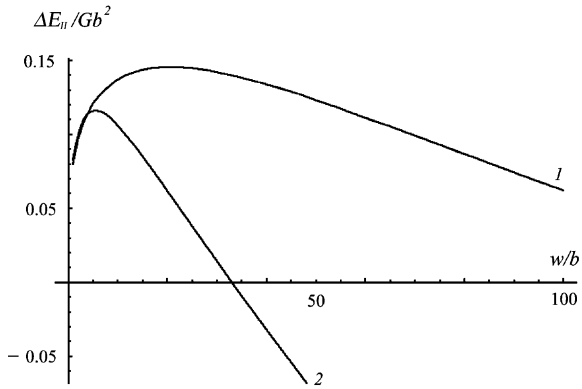

Fig. 6. The energy difference ΔE_{II} via the path w of gliding dislocation in the case of $n = 5$ (1) and 20 (2) dislocations in the initial pile-up under the external shear stress $\tau/G = 0.002$, for the Burgers vector orientations $\alpha_1 = \alpha_2 = \alpha = 50°$.

w_{cII} on parameters of the system are presented in Fig. 7. The solid curves correspond to the symmetric case with $\alpha_1 = \alpha_2 = \alpha$, while the dashed curves to the asymmetric case with $\alpha_1 \neq \alpha_2$. Values of E_{mII} and w_{cII} are lower in the asymmetric cases as compared to those in the symmetric cases with the same values of $\alpha = (\alpha_1 + \alpha_2)/2$. Fig. 7 is indicative of the fact that both the E_{mII} and w_{cII} increase with raising the angles α_1 and α_2.

The comparison between variants (I) and (II) allows us to conclude that the variant (I) is more energetically favourable than variant (II) with the same values of the characteristic parameters. However, the parameters α_1 and α_2 in variant (II) are more flexible; they characterize the misorientation between the Burgers vectors $\boldsymbol{b}_1$ and $\boldsymbol{b}_2$, but not between the fixed grain boundary planes as in the process (I). As a corollary, in general, both the processes (I) and (II) can be realized at triple junctions in plastically deformed nanocrystalline and polycrystalline materials.

3.3. Process (III) (see Fig. 1e and f)

For $n = 5$, and $\tau/G = 0.0002$, 0.002 and 0.01, the dependences $\Delta E_{III}(w)$ are shown in Fig. 8a and b that correspond to $\alpha_1 = \alpha_2 = \alpha = 20°$ and $\alpha_1 = \alpha_2 = \alpha = 50°$, respectively. Here w denotes the distance moved by the mobile lattice dislocation. These dependences give evidence for the

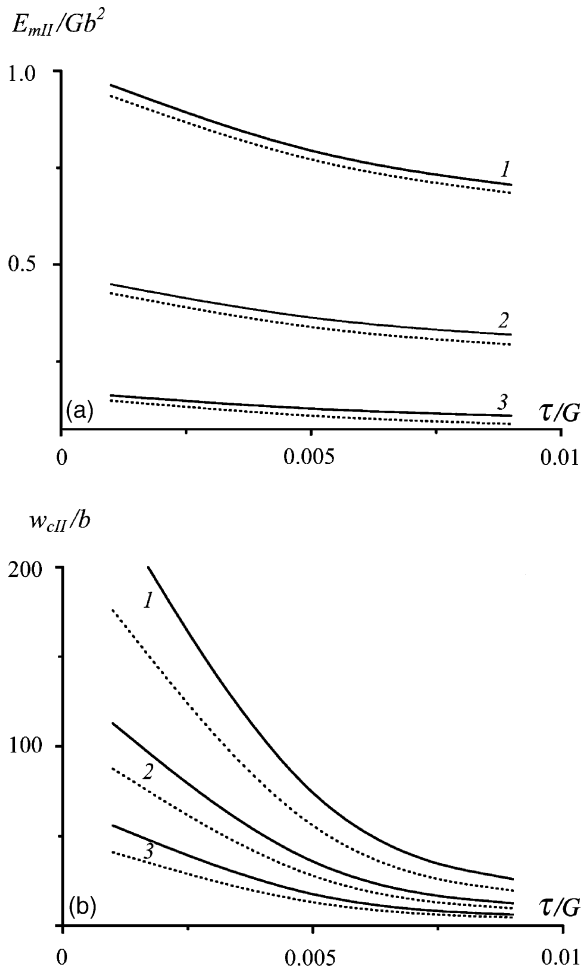

Fig. 7. The energy barrier height ΔE_{III} (a) and the critical distance $\mathbf{w}_{cII}$ (b) via the external shear stress τ for the mean angle $\alpha = (\alpha_1 + \alpha_2)/2 = 60°$ (1), 55° (2), and 50° (3), of the Burgers vector misorientations. The solid lines correspond to the symmetric case with $\alpha_1 = \alpha_2$, while the dashed lines represent the asymmetric case when $\alpha_1 \neq \alpha_2$.

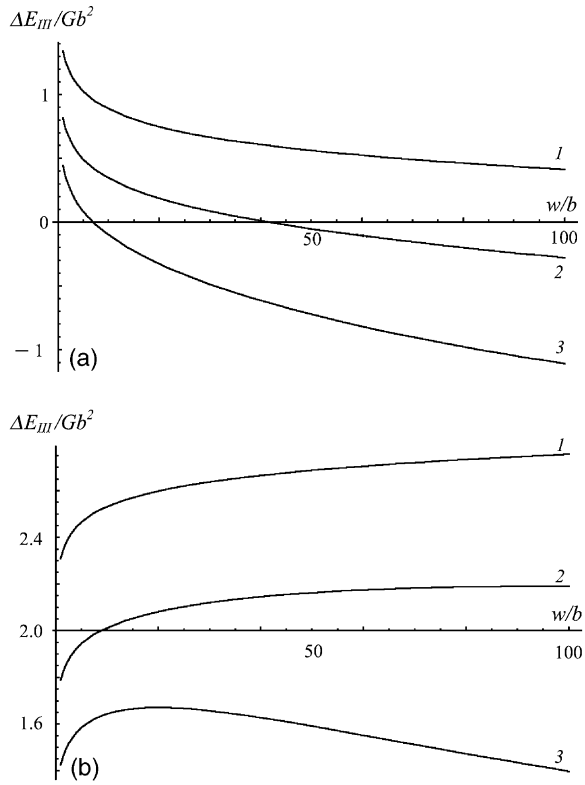

Fig. 8. The energy difference ΔE_{III} via the path $\mathbf{w}$ of gliding dislocation in the case of $n = 5$ dislocations in the initial pile-up under the external shear stress $\tau/G = 0.0002$ (1), 0.002 (2), and 0.01 (3), for the Burgers vector orientations $\alpha_1 = \alpha_2 = \alpha = 20°$ (a) and 50° (b).

barrier type of motion of the mobile lattice dislocation. Moreover, the barrier height E_{mIII} is very high as compared to that in the processes (I) and (II). This allows us to conclude that the process (III) is hardly realized in reality.

3.4. Process (IV) (see Fig. 1g)

The characteristic dependences of ΔE_{IV} on w (where w is the distance moved by the mobile partial dislocation in the grain interior), given by eq. (14), are presented in Fig. 9 for the case of Ag characterized by a very low value of the stacking fault energy ($\gamma \approx 15$ Erg.cm^{-2}). As follows from Fig. 9, the drag force associated with γ plays the important role in hampering the motion of the partial dislocation. In fact, the motion under consideration is energetically unfavourable at realistic values of the parameters of the defect system shown in Fig. 1g.

4. Discussion and concluding remarks

Thus, according to the results of our theoretical analysis, GBD pile-ups may effectively split at triple junctions of grain boundaries in wide ranges of parameters that characterize these defect configurations. GBD pile-ups serve as stress concentrators

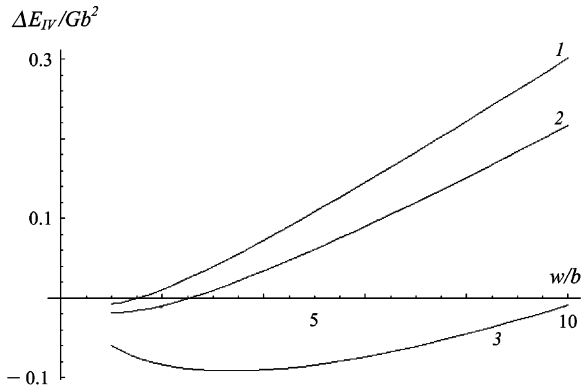

Fig. 9. The energy difference ΔE_{IV} via the path w of gliding dislocation in the case of $n = 30$ dislocations in the initial pile-up under the external shear stress $\tau/G = 0.0002$ (1), 0.002 (2), and 0.01 (3), for the Burgers vector orientations $\alpha_1 = \alpha_2 = \alpha = 20°$ and the stacking fault energy $\gamma = 15$ Erg.cm^{-2}.

[25], in which case the processes of their splitting give rise to a decrease of the stress concentration and, therefore, hamper fracture. In doing so, the geometry of the splitting of GBD pile-ups (Fig. 1b, c and d) strongly influences the grain boundary sliding as a channel of plastic deformation. The splitting of GBD pile-ups effectively occurs at a triple junction of grain boundaries, if its characteristic abutting angles, α_1, and α_2, are low enough (see Section 3). In these circumstances, it is natural to distinguish the so-called "soft" and "hard" triple junctions as those where the dislocation pile-up splitting occurs or does not, respectively, at given conditions of loading (say, a value of the applied mechanical stress). In this context, ratio F_s/F_h of the volume fraction F_S of soft triple junctions to the volume fraction F_h of hard junctions effectively characterizes the contribution of grain boundary sliding to plastic deformation and, therefore, is an important structure-sensitive parameter of the behavior of fine-grained materials under mechanical loading.

Actually, the crossover from the conventional dislocation slip to the deformation mechanisms associated with the active role of grain boundaries (grain boundary sliding [20,21], grain boundary diffusional creep (Coble creep) [27,28], triple junction diffusional creep [29], rotational deformation occurring via motion of grain boundary disclinations [30,31]) is believed to occur in fine-grained materials at small values of grain size d (for a review, see [24]). With results of our theoretical analysis given here, the competition between grain boundary sliding and other deformation mechanisms is crucially influenced by the ratio F_s/F_h characterizing triple junction ensemble. Materials with a high ratio F_s/F_h exhibit enhanced grain boundary sliding characterized by the yield stress value being lower than the yield stress values specifying alternative deformation mechanisms, say, diffusional creep mechanisms. Plastic flow in materials with a low ratio F_s/F_h occurs by alternative deformation mechanism(s), because grain boundary sliding is suppressed.

The suggested representations on soft and hard triple junctions qualitatively account for the experimentally detected difference between the mechanical behaviors of heat-treated and as-fabricated nanocrystalline materials. Thus, a negative slope of Hall–Petch dependence (microhardness or yield stress σ vs $d^{-1/2}$) is exhibited by heat-treated nanocrystalline materials, while as-fabricated nanocrystalline materials are observed to continually strengthen to the smallest grain sizes tested; see [32,33] and references therein. In doing so, heat-treated samples are stronger than as-fabricated ones [32,33]. We think that the difference in question is related to the difference in ratio F_s/F_h between heat-treated and as-fabricated samples. Actually, nanocrystalline materials commonly are synthesized at highly non-equilibrium conditions that cause many GBDs and "non-equilibrium" or, in our terms, soft triple junctions (with dihedral angles between adjacent grain boundaries highly deviating from 120° inherent to "equilibrium" or, in our terms, hard triple junctions) to be generated. In such materials, grain boundary sliding effectively occurs via motion of numerous GBDs that overcome soft triple junctions (as shown in Fig. 1a–d). The reduction of grain size d leads to an increase of the volume fraction of triple junctions which, even if they are soft, hamper grain boundary sliding. Therefore, the strength of as-fabricated materials continually increases with decreasing grain size d. Heat treatment of a nanocrystalline sample results in annihilation of GBDs and transformations of soft ("non-equilibrium") triple junctions into hard ("equilibrium") ones. In our terms,

heat treatment gives rise to an essential decrease of ratio F_s/F_h characterizing triple junction ensemble. As a corollary, grain boundary sliding does not effectively occur in heat treated nanocrystalline materials characterized by low ratio F_s/F_h, in contrast to as-fabricated nanocrystalline materials characterized by high F_s/F_h. This causes heat-treated samples to be stronger than their as-fabricated counterparts. In doing so, grain boundary diffusional creep and/or enhanced triple junction diffusional creep come into play in heat-treated materials, that, according to theoretical models [27–29] are responsible for a negative slope of the Hall–Petch dependence experimentally detected in such materials.

Following experiments [22], the grain boundary sliding in plastically deformed samples induces local migration of grain boundaries, which decreases the characteristic angle α_1 (or α_2) of triple junctions. That is, the grain boundary sliding is capable of transforming hard triple junctions into soft ones, thus facilitating the sliding itself in plastically deformed nanocrystalline and polycrystalline materials. The effects of triple junctions on the deformation behavior and the migration-assisted transformations of hard triple junctions into soft ones account for the plastic flow localization experimentally observed [34–38] in nanocrystalline materials. Actually, in the situation where grain boundary sliding dominates, the difference between homogeneous and inhomogeneous regimes of plastic deformation in as-fabricated nanocrystalline materials is naturally explained as that associated with the behavior of GBD pile-ups at triple junctions. If the mean characteristic ratio F_s/F_h is intermediate, the grain boundary sliding occurs in only some local regions where local value of F_s/F_h is comparatively high. In doing so, the grain boundary sliding induces transformations of hard triple junctions into soft ones due to local migration of grain boundaries in these regions, thus intensifying localization of plastic flow. In other terms, the grain boundary sliding occurs as a self-supporting percolation process in some local regions, in which case a deformed sample exhibits the inhomogeneous deformation regime with plastic flow being localized in shear bands. If the mean ratio F_s/F_h is high, the grain boundary sliding effectively occurs within the mechanically loaded sample as a whole, causing homogeneous plastic deformation.

With the influence of triple junctions on plastic flow localization, we expect that the ability of an as-fabricated nanocrystalline material to exhibit homogeneous or inhomogeneous plastic flow is sensitive to mode of its preparation. For instance, nanocrystalline materials prepared by crystallization of amorphous solids have more equilibrium structure as compared to nanocrystalline materials prepared by highly non-equilibrium methods, say, severe plastic deformation. Therefore, we expect "equilibrium" and "non-equilibrium" nanocrystalline materials (with intermediate and high ratio F_s/F_h, respectively) in their as-fabricated states to exhibit mostly inhomogeneous and homogeneous plastic deformation, respectively. This statement is worth being taken into account in analysis of the experimentally observed [39,40] phenomenon of high strain rate superplasticity — the ability of a solid to undergo large deformation often without the formation of a neck prior to fracture — in nanocrystalline materials produced by severe plastic deformation.

To summarize, in this paper we have theoretically described the role of triple junctions as obstacles for plastic flow occurring via grain boundary sliding. With results of our theoretical analysis, triple junctions strongly influence plastic deformation processes, causing selection of the dominant deformation mechanism realized in mechanically loaded nanocrystalline materials where the volume fraction of the grain boundary phase is extremely high. It is important for understanding the fundamentals of plastic deformation processes in nanocrystalline materials as well as for development of technologies based on plastic forming of nanostructures.

Acknowledgements

This work was supported, in part, by the Office of US Naval Research (grant N00014-01-1-1020), the Russian Fund of Basic Research (grant 01-02-16853), "Integration" Program (grant B0026), and the Russian Research Program on Solid-State Nanostructures.

Appendix A

Let us calculate the energies E_1^{int}, E_2^{int} and E_{1-2}^{int} that characterize interactions between dislocations having non-parallel Burgers vectors (for details, see Section 2). As an example, calculations for the term E_1^{int} are given below in detail. As the calculation procedures for E_2^{int} and E_{1-2}^{int} are absolutely similar, we give only the final results for them.

Following the general method [41], the energy E_1^{int} of the interaction between two dislocations with the Burgers vectors $\boldsymbol{b}'$ and $\boldsymbol{b}''$ is calculated as the work spent to generation of the dislocation with the Burgers vector $\boldsymbol{b}''$ in the stress field of the dislocation with the Burgers vector $\boldsymbol{b}'$. That is,

$$E^{\text{int}} = b''\int_{\infty}^{x_d}\sigma_{xy}^{b'}dx, \tag{A1}$$

where x_d is a parameter characterizing the distance between the dislocations. The energy E_1^{int} may be calculated as a sum of such energies of pair interaction (the energies of interaction between the $\boldsymbol{b}_1$ dislocation and the pile-up dislocations) as follows:

$$E_1^{\text{int}} = \sum_{i=2}^{n} E_{b_1-b_i}^{\text{int}}, \tag{A2}$$

where $E_{b_1-b_i}^{\text{int}}$ is the energy of interaction between the $\boldsymbol{b}_1$ dislocation and the ith dislocation from the pile-up.

For example, let us calculate the energy of interaction between the $\boldsymbol{b}_1$ dislocation and the second dislocation (in the initial pile-up, $i = 2$) having the Burgers vector $\boldsymbol{b}$ (Fig. 10). To do so, it is convenient to write the stress tensor σ_{ij} of the second dislocation in the Oxy coordinate system (Fig. 10) with the x-axis being parallel to the gliding plane of the $\boldsymbol{b}_1$ dislocation. The σ_{xy} component reads

$$\sigma_{xy} = \sigma_{x'y'}\cos 2\alpha_1 + \frac{\sin 2\alpha_1}{2}(\sigma_{y'y'} - \sigma_{x'x'}), \tag{A3}$$

where $\sigma_{x'y'}$, $\sigma_{y'y'}$ and $\sigma_{x'x'}$ are the stress components of the second dislocation in the $Ox'y'$coordinate system which are given by [25]

$$\sigma_{x'x'} = -Db\frac{y'(3x'^2 + y'^2)}{(x'^2 + y'^2)^2},\ \sigma_{y'y'} = Db\frac{y'(x'^2 - y'^2)}{(x'^2 + y'^2)^2},\ \sigma_{x'y'} = Db\frac{x'(x'^2 - y'^2)}{(x'^2 + y'^2)^2} \tag{A4}$$

with

$$x' = x\cos\alpha_1 - y\sin\alpha_1,\ y' = x\sin\alpha_1 + y\cos\alpha_1. \tag{A5}$$

Substitution of eq. (A3) with (A4) and (A5) into (A1) gives

$$E_{b_1-b}^{\text{int}} = b_1\int_{\infty}^{x_d}\left\{\sigma_{xy}(x,y_d)\cos 2\alpha_1 + \frac{\sin 2\alpha_1}{2}[\sigma_{yy}(x,y_d) - \sigma_{xx}(x,y_d)]\right\}dx, \tag{A6}$$

where $x_d = w + x_2\cos\alpha_1$ and $y_d = -x_2\sin\alpha_1$ (Fig. 10). After integration in eq. (A6), we obtain:

$$E_{b_1-b}^{\text{int}} = Dbb_1\left\{\frac{\cos\alpha}{2}\ln\frac{R^2}{x_d^2 + y_d^2} - \frac{y_d(x_d\sin\alpha + y_d\cos\alpha)}{x_d^2 + y_d^2}\right\}. \tag{A7}$$

The energy E_1^{int} is given by a sum (eq. (A2)) of terms similar to $E_{b_1-b}^{\text{int}}$ presented by eq. (A7).

Appendix B

Dislocation positions within a discrete pile-up can be calculated effectively using the theory of the Laguerre polynoms [26]. The Laguerre polynom $L_n(x)$ is defined as the solution of the following equation:

$$x^2\frac{d^2y}{dx^2} + (1-x)\frac{dy}{dx} + ny = 0. \tag{B1}$$

The first derivative $L'_n(x)$ of the Laguerre polynom is the solution of the equation:

$$x\frac{d^2y}{dx^2} + (2-x)\frac{dy}{dx} + (n-1)y = 0. \tag{B2}$$

With eq. (B2), $L'_n(x)$ can be written as follows:

$$L'_n(x) = -\sum_{k=0}^{n-1}\frac{n!(-x)^k}{k!(k+1)!(n-k-1)!}. \tag{B3}$$

As was shown in [26], the roots of the $L'_n(x)$ coincide with dislocation positions in a discrete pile-up.

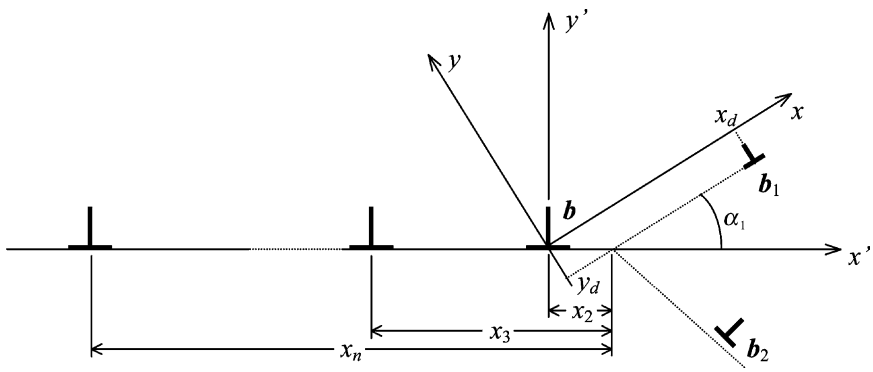

Fig. 10. Schematics of splitting of the head dislocation of a pile-up. The coordinates of the $\boldsymbol{b}_1$ dislocation are $x_d = w + x_2\cos\alpha_1$, and $y_d = -x_2\sin\alpha_1$, where w is the dislocation path after the splitting.

References

[1] Padmanabhan KA, Davies GJ. Superplasticity. Berlin: Springer, 1980.
[2] Pilling J, Ridle N. Superplasticity in crystalline solids. London: The Institute of Metals, 1989.
[3] Sutton AP, Balluffi RW. Interfaces in crystalline materials. Oxford: Clarendon Press, 1995.
[4] Hirth JP. Acta Mater. 2000;48:93.
[5] Valiev RZ, Langdon TG. Acta Metall. 1993;41:949.
[6] Zelin MG, Mukherjee AK. Mater. Sci. Eng. A 1996;208:210.
[7] Zelin MG, Mukherjee AK. J. Mater. Res. 1995;10:864.
[8] Jain M, Christman T. Acta metall. mater. 1994;42:1901.
[9] Mishra RS, Valiev RZ, Mukherjee AK. Nanostruct. Maters. 1997;9:473.
[10] Mayo MJ. Nanostruct. Mater. 1997;9:717.
[11] Zelin MG, Krasilnikov NA, Valiev RZ, Grabski MW, Yang HS, Mukherjee AK. Acta metall. mater. 1994;42:119.
[12] Zelin MG, Mukherjee AK. Acta metall. mater. 1995;43:2359.
[13] Palumbo G, Erb U, Aust KT. Scr. Metall. Mater. 1990;24:2347.
[14] Kornelyuk LG, Lozovoi AYu, Razumovskii IM. Philos. Mag. A 2000;77:465.
[15] Gutkin MYu, Ovid'ko IA. Phys. Rev. B 2001;63:064515.
[16] Gutkin MYu, Ovid'ko IA. Philos. Mag. A 1994;70:561.
[17] Ovid'ko, I.A., In: Chow G-M, Ovid'ko IA, Tsakalakos T, editors. Nanostructured Films and Coatings. NATO Science Series. Dordrecht: Kluwer; 2000, p. 231–246.
[18] Bobylev SV, Ovid'ko IA, Sheinerman AG. Phys. Rev. B 2001;64:224507.
[19] King AH. Interf. Sci. 1999;7:251.
[20] Hahn H, Mondal P, Padmanabhan KA. Nanostruct. Mater. 1997;9:603.
[21] Konstantinidis DA, Aifantis EC. Nanostruct. Mater. 1998;10:1111.
[22] Astanin VV, Sisanbaev AV, Pshenichnyuk AI, Kaibyshev OA. Scr. Mater. 1997;36:117.
[23] Owusu-Boahen K, King AH. Acta Mater. 2001;49:237.
[24] Gutkin MYu, Ovid'ko IA, Pande CS. Rev. Adv. Mater. Sci. 2001;2:80.
[25] Hirth JP, Lothe J. Theory of dislocations. New York: Wiley, 1982.
[26] Eshelby JD, Frank FC, Nabarro FRN. Phil. Mag. 1951;42:351.
[27] Masumura RA, Hazzledine PM, Pande CS. Acta Mater. 1998;46:4527.
[28] Kim HS, Estrin Y, Bush MB. Acta Mater. 2000;48:493.
[29] Fedorov AA, Gutkin MYu, Ovid'ko IA. Scr. Mater. 2002;47:51.
[30] Gutkin MYu, Kolesnikova AL, Ovid'ko IA, Skiba NV. J. Metast. Nanocryst. Mater. 2002;12:47.
[31] Ovid'ko IA. Science 2002;295:2386.
[32] Weertman JR, Sanders PG. Solid State Phenom. 1994;35/36:249.
[33] Volpp T, Göring E, Kuschke W-M, Arzt E. Nanostruct. Mater 1997;8:855.
[34] Niemann GW, Weertman JR, Siegel RW. J. Mater. Res. 1991;6:1012.
[35] Witney AB, Sanders PG, Weertman JR, Eastman JA. Scr. Metall. Mater. 1995;33:2025.
[36] Carsley JE, Milligan WW, Hackney SA, Aifantis EC. Metall. Mater. Trans. A 1995;26:2479.
[37] Andrievskii RA, Kalinnikov GV, Kobelev NP, Soifer YaM, Shtansky D. Phys. Sol. State 1997;39:1661.
[38] Andrievskii RA. In: Chow G-M, Noskova NI, editors. Nanostructured materials: science and technology. Dordrecht: Kluwer Academic Publ; 1998. p. 263–82.
[39] McFadden SX, Mishra RS, Valiev RZ, Zhylyaev AP, Mukherjee AK. Nature 1999;398:684.
[40] Mohamed FA, Li Y. Mater. Sci. Eng. A 2001;298:1.
[41] Mura T. In: Herman H, editor. Advances in material research, vol. 3. New York: Interscience; 1968. p. 1–108.